Multibody Syst Dyn (2007) 17:71–96
DOI 10.1007/s11044-006-9034-2

Simulation model of general human and humanoid motion

Miomir Vukobratović · Veljko Potkonjak · Kalman Babković · Branislav Borovac

Received: 27 January 2006 / Accepted: 28 December 2006

Abstract In the last decade we have witnessed a rapid growth of *Humanoid Robotics*, which has already constituted an autonomous research field. *Humanoid robots* (or simply *humanoids*) are expected in all situations of humans' everyday life, "living" and cooperating with us. They will work in services, in homes, and hospitals, and they are even expected to get involved in sports. Hence, they will have to be capable of doing diverse kinds of tasks. This forces the researchers to develop an appropriate mathematical model to support simulation, design, and control of these systems. Another important fact is that today's, and especially tomorrow's, humanoid robots will be more and more humanlike in their shape and behavior. A dynamic model developed for an advanced humanoid robot may become a very useful tool for the dynamic analysis of human motion in different tasks (walking, running and jumping, manipulation, various sports, etc.). So, we derive a general model and talk about a human-and-humanoid simulation system. The basic idea is to start from a human/humanoid considered as a free spatial system ("flier"). Particular problems (walking, jumping, etc.) are then considered as different contact tasks – interaction between the flier and various objects (being either single bodies or separate dynamic systems).

Keywords Humanoid Robotics · Flier dynamics · Walking · Jumping · Link motion contact · Takeoff · Landing · Contact force · Goalkeeper · Biological modeling

M. Vukobratović
Institute "Mihajlo Pupin", Volgina 15, 11000 Belgrade, Serbia & Montenegro
e-mail: vuk@robot.imp.bg.ac.yu

V. Potkonjak
Faculty of Electrical Engineering, University of Belgrade, Bulevar Kralja Aleksandra 73, 11000 Belgrade, Serbia & Montenegro
e-mail: potkonjak@yahoo.com

K. Babković · B. Borovac
Faculty of Technical Sciences, University of Novi Sad, Trg Dositeja Obradovića 6, 21000 Novi Sad, Serbia & Montenegro
e-mail: bkalman@uns.ns.ac.yu, borovac@uns.ns.ac.yu

1 Introduction: Principles and background

The rapid growth of *Humanoid Robotics* has promoted this branch of robotics to an autonomous research field. *Humanoid robots* (or simply *humanoids*) are expected in all situations of everyday life of humans, to be "living" and cooperating with us. They will work in services, in homes and hospitals, restaurants, etc. It might look surprising, but humanoid robots are expected to get involved even in sports. In 2000, it was proposed that a soccer match could be arranged in 50 years, between a team of robots and the actual world champions. The match was scheduled for 2050 [1]. So, humanoid robots will be capable of doing diverse kinds of tasks. This fact forces the researchers to develop appropriate mathematical models to support simulation, design, and control of these systems.

It is a fact that today's, and especially tomorrow's humanoid robots will be more and more humanlike in their shape and behavior. In [2], it was stated that advanced humanoids should feature human-like motion, humanlike intelligence, and human-like communication. Thus, a sophisticated dynamic model developed for an advanced humanoid robot can be used as a very useful tool for the dynamic analysis of human motion in different tasks (walking, running and jumping, manipulation, different sports, etc.). With this in mind we derive a general model and talk about a human-and-humanoid simulation system.

The authors are well aware of the extreme complexity of the problem of modeling biological systems, which stems from the complexity of the mechanical structure and actuation. Because of that, the authors start with the dynamic modeling of the structure of humanoid robots, which yields a solid approximation of dynamics of the mechanical aspect of human motion. The simulation of a truly biological structure is expected as the next step.

The basic idea of the suggested simulation method is to start from a human/humanoid considered as a free spatial system ("flier"). Particular problems (walking, jumping, etc.) are seen as different contact tasks – interaction between the flier and different objects (in the form of either single bodies or separate dynamic systems). This new idea, proposed in [3], was called "deductive approach." It was checked on some examples in [4]. Let us answer the question: What is the main difference with respect to the previous results in human/humanoid dynamics?

Researchers in biomechanics and robotics have devoted great efforts to investigate different problems in motion of humans and humanoid robots. We mention only a few illustrative examples. Bipedal gait has widely been elaborated [5–7]. Jumping and running have been solved recently [8]. A very different model was developed for a rather different motion – somersaults on the trampoline [9, 10]. A review of advanced topics in humanoid dynamics can be found in [11]. One may note that for these particular problems, separate models were developed. If specific models were derived for different problems, like gymnastic exercise, soccer or tennis [12, 13], then it would be a huge problem to make a generalization. Our approach (initiated in [3, 4]) follows a deductive principle; we derive a general model and consider all mentioned particular motions as being just special cases. Contact analysis, essential in this method, follows the theory explained in [14].

According to [3], the general approach is based on an *articulated system* (e.g. a human body, a humanoid, or even an animal) that "flies" without constraints (meaning that it is not connected to the ground or to any object in its environment – see Figure 1). The term *flier* was suggested. Such situation is not uncommon in reality (it is present in running, jumping, trampoline exercise, etc.), but it is less common than the motion where the system is in contact with the *ground* or some other supporting *object* in its environment (e.g., single- and double-support phases of walking, gymnastics on some apparatus, etc.).

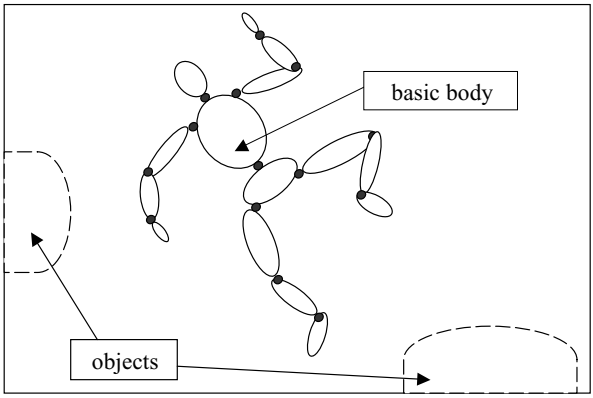

Fig. 1 Unconstrained system – free flier

Let us discuss the contact of the flier and some external *OBJECT* (the term *object* includes the ground). A contact can be *rigid* or *soft*. With a rigid contact, one *LINK* (or more of them) of the flier is geometrically constrained in its motion. An example is the gait, where the foot is in contact with a nondeformable support. With a soft contact, there is no geometric constraint imposed on the system motion, but the strong elastic forces between the contacted link and some external object make the link motion close to the object. Two examples of such contact are walking on a support covered with elastic layer, and trampoline exercise.

Let us recall some additional justification of the *flier-plus-contact approach*. A human is strongly related with the ground (or any kind of support). He usually needs the ground in order to "feel" his own position. It is desirable that there is a physical contact with the ground, or at least a visual contact. However, a trained human (in gymnastics, trampoline exercise, somersaults, different ball playing, circus performance on the trapeze, etc.) is ready to see himself as a flier. He can feel his position in space – the ground loses its importance. Such humans can concentrate on the contact that is expected. It becomes possible to keep the eyes on the object that is to be contacted, and thus concentrate just on this relative position. The object may be immobile (e.g. the ground or a gymnastic horse) or moving (e.g., a ball).

As mentioned above, the system is modeled as a robot. This means that it involves joints that have one degree of freedom (DOF) each. More complex joint, like human shoulder for example, are modeled as a series of one-DOF connections. The algorithm and the developed software allow revolute or linear joints. The presented examples include just revolute connections. The complexity of the system is theoretically arbitrary – the software works for any input number of DOFs. The complexity is always chosen so as to be appropriate to the motion task and the analysis required. This complex robotic structure is seen as an approximation of a human body. Generally speaking, there is no obstacle to model the geometry of a truly biological structure. The drives, however, introduce problems – muscles are rather different from robot actuators. It is our opinion that if the entire body was modeled in a "biological way" the system would become unnecessarily complex. So, the next step of work will be to identify the "key joints" for a particular action (for instance, in tennis these are arm joints) and model them respecting their truly biological structure. The others will still be "robotic" (thus approximate).

2 Free-flier motion

We consider a flier as an articulated system consisting of the *basic body* (the torso) and several *branches* (head, arms, and legs), as shown in Figure 1. Let there be n independent joint motions

described by joint-angles vector $\mathbf{q} = [q_1, \ldots, q_n]^T$. (The terms *joint coordinates* or *internal coordinates* are often used.) The basic body needs six coordinates to describe its spatial position: $\mathbf{X} = [x, y, z, \theta, \varphi, \psi]^T$, where x, y, z defines the position of the mass center and θ, φ, ψ are orientation angles (roll, pitch, and yaw). Now, the overall number of DOFs for the system is $N = 6 + n$, and the system position is defined by

$$\mathbf{Q} = [\mathbf{X}^T, \mathbf{q}^T]^T = [x, y, z, \theta, \varphi, \psi, q_1, \ldots, q_n]^T \tag{1}$$

We now consider the drives. It is assumed that each joint motion q_j has its own drive–the torque τ_j. Note that in this analysis there is no drive associated to the basic-body coordinates $\mathbf{X}$.[1] The vector of the joint drives is $\boldsymbol{\tau} = [\tau_1, \ldots, \tau_n]^T$, and the extended drive vector (N-dimensional) is $\mathbf{T} = [0_6, \boldsymbol{\tau}^T]^T = [0, \ldots, 0, \tau_1, \ldots, \tau_n]^T$.

The dynamic model of the flier has the general form:

$$\mathbf{H}(\mathbf{Q})\ddot{\mathbf{Q}} + \mathbf{h}(\mathbf{Q}, \dot{\mathbf{Q}}) = \mathbf{T} \tag{2}$$

or

$$\begin{aligned} \mathbf{H}_{X,X}\ddot{\mathbf{X}} + \mathbf{H}_{X,q}\ddot{\mathbf{q}} + \mathbf{h}_X &= \mathbf{0} \\ \mathbf{H}_{q,X}\ddot{\mathbf{X}} + \mathbf{H}_{q,q}\ddot{\mathbf{q}} + \mathbf{h}_q &= \boldsymbol{\tau} \end{aligned} . \tag{3}$$

Dimensions of the inertial matrix and its submatrices are: $\mathbf{H}(N \times N)$, $\mathbf{H}_{X,X}(6 \times 6)$, $\mathbf{H}_{X,q}$ $(6 \times n)$, $\mathbf{H}_{q,X}(n \times 6)$, and $\mathbf{H}_{q,q}(n \times n)$. Dimensions of the column vectors containing centrifugal, Coriolis' and gravity effects are: $\mathbf{h}(N)$, $\mathbf{h}_X(6)$, and $\mathbf{h}_q(n)$.

3 Link motion and contact

Let us consider a *LINK* that has to establish a contact with some external *OBJECT*. In one example, it is the foot moving toward the ground and ready to touch it (in walking or running). In the next example, in a soccer game, one may consider the foot or the head moving toward a ball in order to hit. The external object may be immobile (like the ground), an individual moving body (like a ball), or a part of some other complex dynamic system (even another flier, like in a trapeze exercise in the circus). Note that the contact might be an inner one – involving two links of the considered system, an example being the tennis player holding the racket with both hands.

In order to express the coming contact mathematically, we describe the motion of the considered link by an appropriate set of coordinates. Since the link is a body moving in space, it is necessary to use six coordinates. Let this set be $\mathbf{s} = [s_1, \ldots, s_6]^T$, and let us call them *functional coordinates* (often referred to as s-coordinates). Functional coordinates are introduced as relative ones, defining the position of the link with respect to the object to be contacted. Several illustrative examples of s-coordinates were shown in [3]. Each choice was made in accordance with the expected contact – to support its mathematical description.

[1] This is a real situation with humans and humanoids in "normal" activities. However, humans are already engaged in space activities and humanoids are expected soon (actions alike repairing a space station, etc.) to be doing the same. In such activities, reactive drives are added, and they are attached to the torso. The proposed method for simulation can easily handle this situation.

A consequence of the rigid link-object contact is that the link and the object perform some motions, along certain axes, together. These are *constrained* (*restricted*) *directions*. Let there be m such directions, m being a characteristic of a particular contact. Relative position along these axes does not change. Along other axes, relative displacement is possible. These are *unconstrained* (*free*) *directions*. In order to get a simple mathematical description of the contact, s-coordinates are introduced so as to describe relative position. Zero value of some coordinate indicates the contact along the corresponding axis. For a better understanding, we use a well-known example – the contact of the robot foot and the ground (Figure 2). We may distinguish several situations. The heel contact (Figure 2a) restricts five s-coordinates, leaving one free (thus, $m = 5$). The full-foot contact (Figure 2b) restricts all six coordinates ($m = 6$). Finally, if the robot is falling down by rotating about the foot edge (Figure 2c), then again $m = 5$.

The motion of the external object (to be contacted) has to be known (or calculated from the appropriate mathematical model), and then the s-frame fixed to the object is introduced to describe the relative position of the link in the most proper way. In the case of an inner contact (two links in contact), one link has to play the role of the object. Thus, in a general case, the s-frame is mobile. As the link is approaching the object, some of the s-coordinates reduce and finally reach zero. The zero value means that the contact is established. These functional coordinates (which reduce to zero) are called *restricted coordinates* and they form the subvector $\mathbf{s}^c$ of dimension m. The other functional coordinates are *free* and they form the subvector $\mathbf{s}^f$ of dimension $6 - m$. Now one may write:

$$\left[\mathbf{s}^{c^T}, \quad \mathbf{s}^{f^T}\right]^T = \mathbf{s} \quad \text{or} \quad \left[\mathbf{s}^{c^T}, \quad \mathbf{s}^{f^T}\right]^T = \mathbf{K}\,\mathbf{s} \tag{4}$$

where $\mathbf{K}$ is a 6×6 matrix used, when necessary, to rearrange the functional coordinates (elements of the vector $\mathbf{s}$) and bring the restricted ones to the first position.

Note that there are several types of possible contacts between the two bodies. One contact will restrict some s-coordinates while the other will restrict a different set. Different links may establish a contact. In different tasks, the same link will establish different contacts with different objects. For each example, a specific s-frame is needed. So, in order to arrive at a general algorithm, we have to describe link motion in a general way and, once the expected contact is specified, relate this general interpretation to the appropriate s-frame.

The general description of the link motion assumes the three Cartesian coordinates of a selected point of the link plus the three orientation angles: $\mathbf{X}_l = [x_l, y_l, z_l, \theta_l, \varphi_l, \psi_l]^T$, the subscript l standing for "*l*ink." These are absolute external coordinates. The relation between the link coordinates $\mathbf{X}_l$ and the system position vector $\mathbf{Q}$ is straightforward:

$$\mathbf{X}_l = \mathbf{X}_l(\mathbf{Q}) \tag{5}$$

$$\dot{\mathbf{X}}_l = \mathbf{J}_l(\mathbf{Q})\dot{\mathbf{Q}} \tag{6}$$

$$\ddot{\mathbf{X}}_l = \mathbf{J}_l(\mathbf{Q})\ddot{\mathbf{Q}} + \mathbf{A}_l(\mathbf{Q}, \dot{\mathbf{Q}}) \tag{7}$$

where $\mathbf{J}_l = \partial\mathbf{X}_l/\partial\mathbf{Q}$ is a $6 \times N$ Jacobian matrix and $\mathbf{A}_l = \partial^2\mathbf{X}_l/\partial\mathbf{Q}^2\dot{\mathbf{Q}}^2$ is a 6×1 adjoint matrix (6-component column vector).

Let us concentrate on the object. In different examples, the same object will be contacted in different ways (e.g., in handball, the hand grasps the ball, while in volleyball the hand hits the ball). Now, consider the ground (as an example of an immobile object); in walking, one

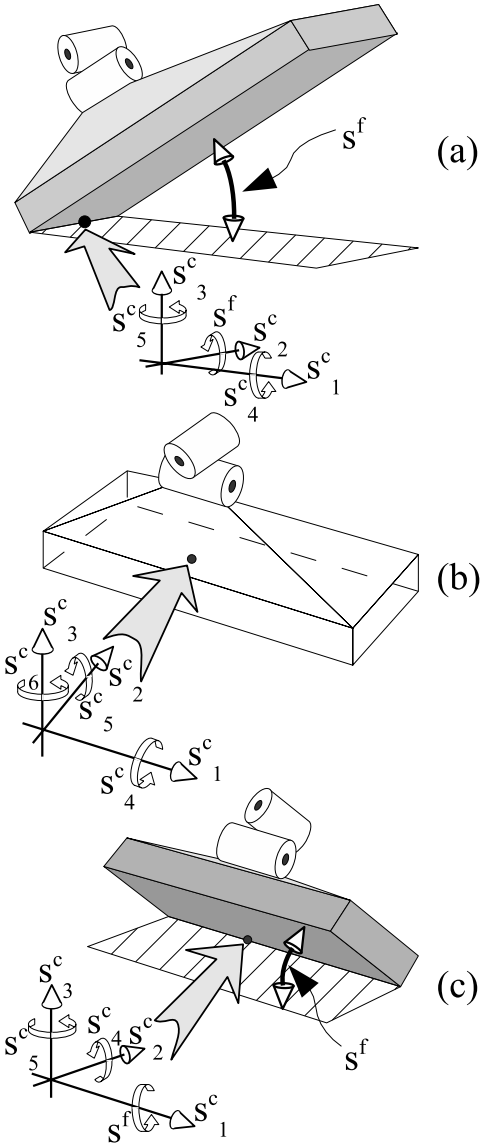

Fig. 2 Different contacts of the humanoid foot and the ground. The superscript "c" indicates constrained (restricted) coordinates, while "f" indicates the free ones. (a) The heel contact restricts five *s*-coordinates, leaving one free. (b) The full-foot contact restricts all six coordinates. (c) If the robot is falling down by rotating about the foot edge, then there is again one free coordinate

type of contact of the foot and the ground exists, while in ice-skating the contact will be of a rather different kind. In a general case, the object is mobile, so, its position is described by the absolute external coordinates: $\mathbf{X}_b = [x_b, y_b, z_b, \theta_b, \varphi_b, \psi_b]^T$, the subscript b standing for "object."

When the *s*-frame is introduced to define the relative position of the link with respect to the object, the coordinates will depend on both $\mathbf{X}_b$ and $\mathbf{X}_l$:

$$\mathbf{s} = \mathbf{s}(\mathbf{X}_l, \mathbf{X}_b) \tag{8}$$

or in the Jacobian form:

$$\dot{\mathbf{s}} = \mathbf{J}_{sl}\dot{\mathbf{X}}_l + \mathbf{J}_{sb}\dot{\mathbf{X}}_b \tag{9}$$

$$\ddot{\mathbf{s}} = \mathbf{J}_{sl}\ddot{\mathbf{X}}_l + \mathbf{J}_{sb}\ddot{\mathbf{X}}_b + \mathbf{A}_s. \tag{10}$$

where dimension of all Jacobi matrices is 6×6, and the dimension of the adjoint vector $\mathbf{A}_s$ is 6×1.

Model (10) can be rewritten if the separation (4) is introduced. The model becomes

$$\ddot{\mathbf{s}}^c = \mathbf{J}^c_{sl}\ddot{\mathbf{X}}_l + \mathbf{J}^c_{sb}\ddot{\mathbf{X}}_b + \mathbf{A}^c_s \tag{11}$$

$$\ddot{\mathbf{s}}^f = \mathbf{J}^f_{sl}\ddot{\mathbf{X}}_l + \mathbf{J}^f_{sb}\ddot{\mathbf{X}}_b + \mathbf{A}^f_s. \tag{12}$$

Suppose that the object motion, $\mathbf{X}_b(t)$ in Equations (8)–(10), is either prescribed or calculated from a separate mathematical model of the object. Equations (11) and (12) can be rewritten if Equation (7) is introduced:

$$\ddot{\mathbf{s}}^c = \mathbf{J}^c_{sl}\mathbf{J}_l\ddot{\mathbf{Q}} + \mathbf{J}^c_{sl}\mathbf{A}_l + \mathbf{J}^c_{sb}\ddot{\mathbf{X}}_b + \mathbf{A}^c_s = \mathbf{J}^c_{s,\mathrm{TOT}}(\mathbf{Q},\, t)\ddot{\mathbf{Q}} + \mathbf{A}^c_{s,\mathrm{TOT}}(\mathbf{Q}, \dot{\mathbf{Q}}, t), \tag{13}$$

$$\ddot{\mathbf{s}}^f = \mathbf{J}^f_{sl}\mathbf{J}_l\ddot{\mathbf{Q}} + \mathbf{J}^f_{sl}\mathbf{A}_l + \mathbf{J}^f_{sb}\ddot{\mathbf{X}}_b + \mathbf{A}^f_s = \mathbf{J}^f_{s,\mathrm{TOT}}(\mathbf{Q},\, t)\ddot{\mathbf{Q}} + \mathbf{A}^f_{s,\mathrm{TOT}}(\mathbf{Q}, \dot{\mathbf{Q}}, t), \tag{14}$$

where the model matrices are: $\mathbf{J}^c_{s,\mathrm{TOT}} = \mathbf{J}^c_{sl}\,\mathbf{J}_l$, $\mathbf{A}^c_{s,\mathrm{TOT}} = \mathbf{J}^c_{sl}\,\mathbf{A}_l + \mathbf{J}^c_{sb}\,\ddot{\mathbf{X}}_b + \mathbf{A}^c_s$, $\mathbf{J}^f_{s,\mathrm{TOT}} = \mathbf{J}^f_{sl}\,\mathbf{J}_l$, $\mathbf{A}^f_{s,\mathrm{TOT}} = \mathbf{J}^f_{sl}\,\mathbf{A}_l + \mathbf{J}^f_{sb}\,\ddot{\mathbf{X}}_b + \mathbf{A}^f_s$

When speaking about a moving object one may distinguish two cases. *The first case assumes that the object motion is given and cannot be influenced by the flier dynamics*. Immobile object is included in this case. Such situation appears if the object mass is considerably larger than the flier mass (so, the flier influence may be neglected), or if the object is driven by so strong actuators that can overcome any influence on the object motion. An example would be walking on the ground, i.e., contact between the foot and the ground. Ground is the large immobile object. Another example is walking on a large ship. The ship is a large object whose motion is practically independent of the walker. The ship is a dynamic system but it cannot be influenced by the walker, and so, from the standpoint of the walker, the ship motion may be considered as given. Equations (13) and (14) apply for this first case.

The other case refers to the object being a "regular" dynamic system, so that the flier dynamics can have an effect on it. The example is a handball player that catches the ball. The ball is an object strongly influenced by the player. The next example is the walking on a small boat. The boat behavior depends on the motion of the walker. For this case, Equations (11) and (12) should be combined with the dynamic equations of the object and solved together.

Division of contacts can be done based on the existence of deformations in the contact zone. If there is no deformation, i.e., if the motions of the two bodies are equal in the restricted directions, then we talk about the *rigid contact*. If deformation is possible, then the motions in the restricted directions will not be equal. Theoretically, they will be independent, but in reality they will be close to each other, due to the action of strong elastic forces. In this case, we talk about the *soft contact*.

Another division of contacts is also necessary. *One class of contacts encompasses durable (lasting) contacts*. This means that the two bodies (link and object), after they touched each other and when the impact is over, continue to move together for some finite time. The example is walking. When the foot touches the ground, it keeps the contact for some time

before it moves up again. The next example is found in handball playing. When the player catches the ball, he will keep it for some time before throwing.

The other class represents the instantaneous, short-lived contacts. When the two bodies touch each other, a short impact occurs, and after that the bodies disconnect. A good example is the volleyball player who hits the ball (with his hand).

It is clear that a general theory of impact, including the elastodynamic effects, can cover all the mentioned contacts. However, the intention of this paper is to demonstrate the feasibility and potentials of the proposed method, and not to explore all the details of impact effects. Thus, the discussion of the contact type is not seen as a primary problem. So, in the present paper, we are going to elaborate in detail one representative type of contact – rigid, durable contact involving the object that moves according to a given law.[2]

4 Analysis of the contact

This section adopts the following:

- *contact is rigid* – allowing no deformation between the two bodies;
- *object motion is given and cannot be influenced by the flier* (thus, $\mathbf{X}_b(t)$ is considered given);
- *contact is durable* – lasting for a finite time after the impact.

One may recognize the three phases of such contact task [3, 4, 14]: approaching, impact, and regular contact motion.

Approaching: The link moves toward the object. All functional coordinates $\mathbf{s}$ are free, but some of them (subvector $\mathbf{s}^c$) gradually reduce to zero.

Impact: In the preceding phase (approaching), the motion of the link could be planned so as to hit the object (like in volleyball or in landing after a jump), or it could be planned so as to reach the object with a relative velocity equal zero (collision-free contact, like in grasping a glass of wine). This is the reference motion. In the first case, the collision (and the impact) is intentional. In the other case, collision is undesired but it still occurs. Namely, the control system produces the actual motion different from the reference; the tracking error leads to the collision, a nonzero-velocity contact. The impact forces will affect the system state – after the impact the link state will comply with the object state and the type of contact. The adopted rigid and durable contact understands an ideally plastic impact.

Regular contact motion: The contact forces make the link move according to the character of the contact.

We now elaborate these phases starting with the first one – approaching. The third phase (regular contact motion) will be discussed before the second phase (impact) since it is more convenient for the mathematical derivation of the models.

4.1 Approaching

From the standpoint of mathematics, approaching is an unconstrained (thus free) motion. Although all coordinates from the vector $\mathbf{s}$ are free, we use the separation (4) since the subvector $\mathbf{s}^c$ is intended to describe the coming contact. Strictly speaking, the restricted coordinates (elements of $\mathbf{s}^c$) reach zero one by one. So, a complex contact is established as

[2] Such contact, as well as the general elastodynamic contact, are explained in [14]. Note that the adopted type of contact understands an ideally plastic impact.

a series of simpler contact effects. Without loss of generality one may assume that all the coordinates $\mathbf{s}^c$ attain zero simultaneously and establish a complex contact instantaneously.

The dynamics of the approaching is described by the model (2). The model represents the set of N scalar equations that can be solved for N scalar unknowns – acceleration vector $\ddot{\mathbf{Q}}$ (thus enabling the integration and calculation of the system motion $\mathbf{Q}(t)$). The link motion in the absolute external frame, $\mathbf{X}_l$, is calculated by using (7). For the approaching phase, it is more interesting to observe functional coordinates. Since the object motion $\mathbf{X}_b$ is given, relation (10) [i.e. (11), (12)] or relations (13) and (14), allow one to calculate the link functional trajectory $\mathbf{s}(t)$.

The reference motion $\mathbf{s}*(t)$ (sign * will be used to denote reference values of a variable) is planned so as to make a zero-velocity contact at the instant t_c^*: $\mathbf{s}^c*(t_c^*)=0$ and $\dot{\mathbf{s}}^c*(t_c^*)=0$. Due to the control system, tracking error will appear and the actual motion $\mathbf{s}$ will differ from the reference. So, it is necessary to monitor the coordinates $\mathbf{s}^c$ and detect the contact as the instant t_c' when $\mathbf{s}^c$ reduces to zero ($\mathbf{s}^c(t_c')=0$). It will be $t_c'\neq t_c^*$, and the actual contact velocity will not be zero: $\dot{\mathbf{s}}^c(t_c')\neq 0$.

During the approaching phase, the integration of the system coordinates $\mathbf{Q}$ is done. So, at the instant of impact, there will be some system state $\mathbf{Q}(t_c')$, $\dot{\mathbf{Q}}(t_c')$.

4.2 Regular contact motion

Regular contact motion starts when the transient effects of the impact vanish. In this phase the restricted coordinates are kept zero. So,

$$\mathbf{s}^c(t)=0 \tag{15}$$

and accordingly

$$\dot{\mathbf{s}}^c(t)=0,\quad \ddot{\mathbf{s}}^c(t)=0. \tag{16}$$

Now, relation (13) is replaced with

$$\mathbf{J}^c_{s,\mathrm{TOT}}(\mathbf{Q},t)\,\ddot{\mathbf{Q}}+\mathbf{A}^c_{s,\mathrm{TOT}}(\mathbf{Q},\dot{\mathbf{Q}},t)=0 \tag{17}$$

while relation (14) still holds:

$$\ddot{\mathbf{s}}^f=\mathbf{J}^f_{s,\mathrm{TOT}}(\mathbf{Q},t)\ddot{\mathbf{Q}}+\mathbf{A}^f_{s,\mathrm{TOT}}(\mathbf{Q},\dot{\mathbf{Q}},\mathbf{t}).$$

In contact problems, the dynamic model has to take care of contact forces. Model (2), derived for a free flier, should be supplemented by introducing contact forces. A contact force acts along each of the constrained axes. So, there is a reaction force (or torque) for each coordinate from the set $\mathbf{s}^c$. There are m independent reactions. Let $\mathbf{F}=[F_1,\ldots,F_m]^T$ be the reaction vector. If a coordinate s_j^c is a linear one (translation) then the corresponding reaction F_j is a force. For a revolute coordinate, the corresponding reaction is a torque.

The contact-dynamics model is obtained by introducing reactions into the free-flier model (2):

$$\mathbf{H}(\mathbf{Q})\ddot{\mathbf{Q}}+\mathbf{h}(\mathbf{Q},\dot{\mathbf{Q}})=\mathbf{T}+\left(\mathbf{J}^c_{s,\mathrm{TOT}}(\mathbf{Q},t)\right)^T\mathbf{F} \tag{18}$$

Since this model involves N scalar equations and $N+m$ scalar unknowns (vectors $\ddot{\mathbf{Q}}$ and $\mathbf{F}$), it is necessary to supply some additional conditions. The additional condition is the

constraint relation (17), containing m scalar equations. So, Equations (17) and (18) describe the dynamics of a constrained flier, allowing one to calculate the acceleration $\ddot{\mathbf{Q}}$ and reaction $\mathbf{F}$ (thus enabling integration of the equations and calculation of the system motion).

4.3 Impact analysis

Let t_c' be the instant when the contact is established (restricted coordinates reduce to zero and the impact comes into action) and let t_c'' be the instant when the impact ends. So, the impact lasts for $\Delta t = t_c'' - t_c'$. For this analysis we adopt the infinitely short impact, i.e., $\Delta t \to 0$. We also assume that the m coordinates (forming $\mathbf{s}_c$) reduce to zero simultaneously.

We now integrate the dynamic model (18) over the short impact interval Δt, obtaining:

$$\mathbf{H}\,\Delta\dot{\mathbf{Q}} = \left(\mathbf{J}^c_{s,\mathrm{TOT}}\right)^T \mathbf{F}\Delta t, \tag{19}$$

where

$$\Delta\dot{\mathbf{Q}} = \dot{\mathbf{Q}}(t_c'') - \dot{\mathbf{Q}}(t_c') = \dot{\mathbf{Q}}'' - \dot{\mathbf{Q}}'. \tag{20}$$

During the approaching phase, the system model was integrated and the motion $\mathbf{Q}(t)$, $\dot{\mathbf{Q}}(t)$ was calculated. Thus, the state at the instant t_c', i.e., $\mathbf{Q}' = \mathbf{Q}(t_c')$, $\dot{\mathbf{Q}}' = \dot{\mathbf{Q}}(t_c')$, is considered known. Since the object motion is also known, it is possible to calculate the model matrices $\mathbf{H}$, $\mathbf{J}^c_{s,\mathrm{TOT}}$ in the Equation (19). The position does not change during $\Delta t \to 0$, and hence:

$$\mathbf{Q}'' = \mathbf{Q}(t_c'') = \mathbf{Q}'. \tag{21}$$

Now, the model (19) contains N scalar equations with $N + m$ scalar unknowns: the change in velocity across the impact, $\Delta\dot{\mathbf{Q}}$ (dimension N), and the impact momentum $\mathbf{F}\Delta t$ (dimension m). Due to the ideally plastic impact, the additional equations needed to allow the solution are obtained by rewriting the constraint relation (17) into the first-order form:

$$\mathbf{J}^c_{s,\mathrm{TOT}}(\mathbf{Q}, t)\dot{\mathbf{Q}}'' = 0 \geq \quad \mathbf{J}^c_{s,\mathrm{TOT}}\ \Delta\dot{\mathbf{Q}} = -\mathbf{J}^c_{s,\mathrm{TOT}}\,\dot{\mathbf{Q}}', \tag{22}$$

that contains m scalar conditions. The augmented set of Equations (19) and (21), allow to solve the impact. The change $\Delta\dot{\mathbf{Q}}$ is found and then Equation (20) enables one to calculate the velocity after the impact (i.e.,$\dot{\mathbf{Q}}'' = \dot{\mathbf{Q}}(t_c'')$). So, the new state (in t_c'') is found starting from the known state in t_c'. The impact momentum $\mathbf{F}\Delta t$ is determined as well. The new state $\mathbf{Q}''$, $\dot{\mathbf{Q}}''$ represents the initial condition for the third phase, the regular contact motion (explained in 4.2).

5 Simulation: General comments

In order to verify the proposed general method and show its potentials, two examples have been selected. Both are from sport. Such choice has been made having in mind the following:

- examples from sports are complex and attractive, and thus suitable to show the potentials of the proposed model;
- the foreseen application of the model and the related software includes sports;
- humanoids are expected in sports.

The intention of this paper is to demonstrate what such dynamic models can do. If it proves to be efficient in dynamic analysis, it will be a useful tool for all who work in biomechanics of sporting motion. Simulation can be used to improve the motion in the sense of getting best

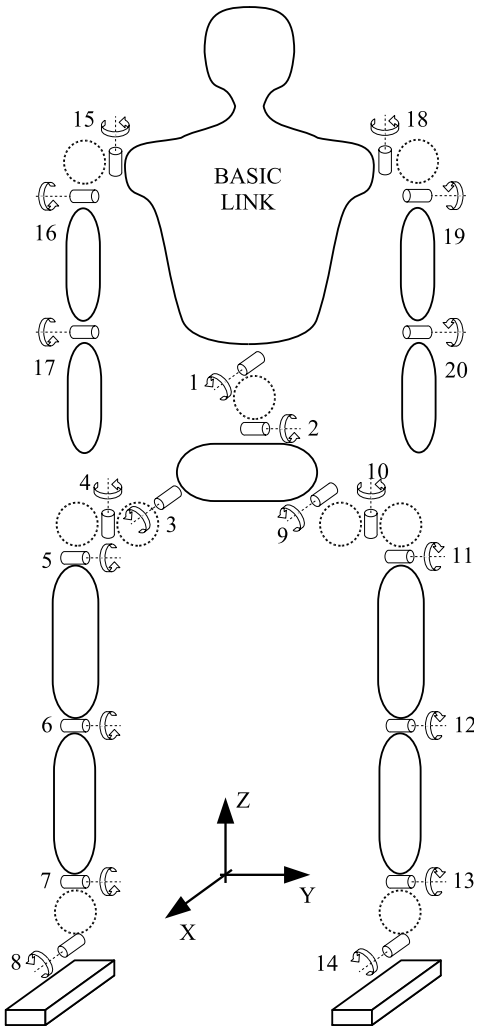

Fig. 3 Adopted configuration of the human/humanoid

from human/humanoid potentials. So, the reference motions of the human/humanoid, which will be used for examples need not be "perfect." From the standpoint of dynamic model, a clumsy (inexperienced) player is as good as a well trained one. Simulation can be used to find a way to improve the motion. Motions in our examples will be similar to some extent to realistic motions of sportsmen in selected disciplines. Motions will not be taken from measurements but numerically generated. In order to prove the model's potentials, it is most important that the chosen motions involve different phases regarding the system structure and the character of motion: open- and closed-chain structures, contact with the ground, free spatial motion, impact, contact with an external dynamic system (e.g., a ball), etc. All different phases will be solved by the software based on the proposed general method.

From the viewpoint of dynamic approach, Newton-Euler formalism was implemented. For geometry and kinematics of the system, the approach based on Rodrigues' formula of finite rotation was used. Initial MATLAB realization of simulation system featured inappropriate time consumption. So, C programming was adopted and simulation experiments performed.

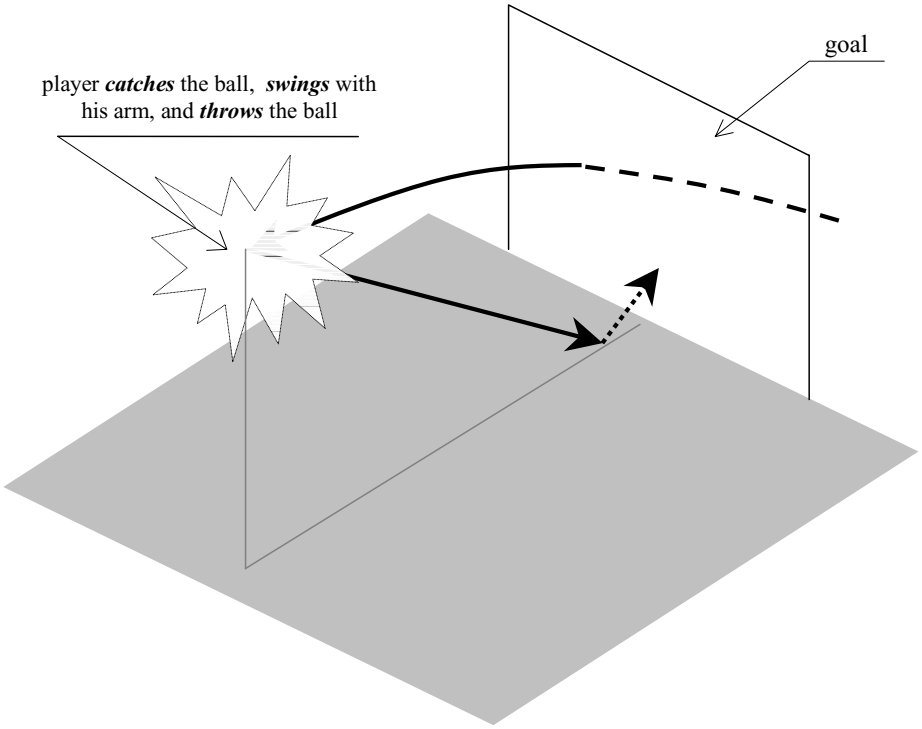

Fig. 4 Required ball motion

6 Simulation: Example 1

6.1 Configuration and the task

We consider a human/humanoid model having $n = 20$ DOFs at its joints, shown in Figure 3. This can be seen as a humanoid or an approximation of human body. Definition of the joint (internal) coordinates, vector $\mathbf{q} = [q_1, \ldots, q_n]^T$, is presented as well. Main parameters of the human/humanoid are given in Appendix. Here, we only mention that its total weight (mass) is ca. 70 kg.

The task is selected as a specific action in handball. A player jumps, catches the ball with his right hand, and throws the ball while still flying. The ball should hit the ground in front of the goalkeeper in order to trick him (Figure 4). In a realistic situation, this would be a learned pattern. So, we consider this player's motion as a reference and try to realize it. As stated above, for the purpose of simulation the reference motion was not measured but synthesized numerically.[3] Here, we do not show the reference; the realized motion is considered a sufficient information. The ball mass is 450 g and the radius is 9.5 cm.

The human/humanoid is equipped with actuators at its joints and the control system will try to track the reference motion. Following the biological principle, the control input in some

[3] Synthesis of the human-like reference motion was mainly done by trial and error. In some foreseen practical implementation of the proposed simulation (dynamic) model, it is expected to use a motion-capture system to record a high-quality reference. For the purpose of demonstrating the potentials of the dynamic model, we consider as enough if the motion roughly looks humanlike.

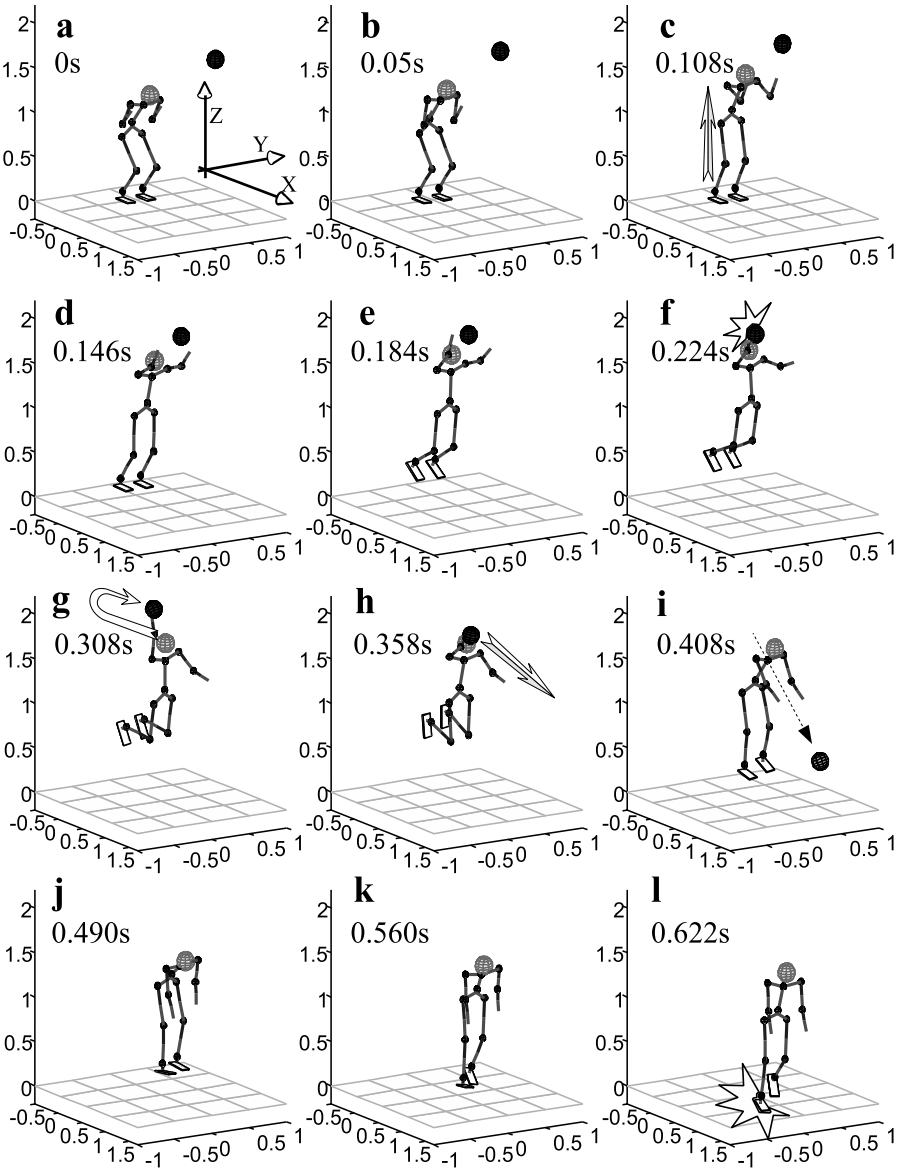

Fig. 5 The "movie" of the human/humanoid player motion. Characteristic instants defining the phases of motion are indicated

joint j consists of the feedforward term and the feedback:

$$\tau_j = \underbrace{\tau_j^*}_{\text{feedforward}} \underbrace{-K_{Pj}(q_j - q_j^*) - K_{Dj}(\dot{q}_j - q_j*)}_{\text{feedback}}, \qquad j = 1, \ldots, n$$

With humans, feedforward is the matter of learning and training. With humanoids, being in fact machines, feedforward is calculated from a mathematical model. Since dynamics, and

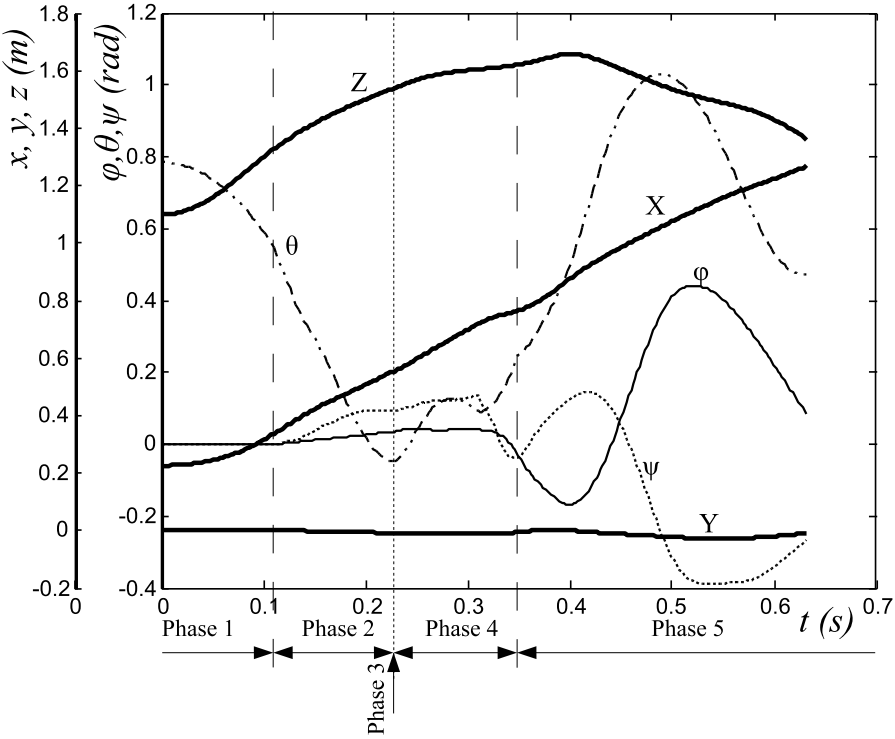

Fig. 6 Time histories of the main-body (torso) coordinates: $x(t)$, $y(t)$, $z(t)$, $\theta(t)$, $\varphi(t)$, $\psi(t)$

not control, is the key point of this paper, we apply a simplified control – a PD regulator:

$$\tau_j = -K_{Pj}(q_j - q_j^*) - K_{Dj}\dot{q}_j, \quad j = 1, \ldots, n.$$

where q_j is the actual value of a joint coordinate, and $q_j^*(t)$ is its prescribed reference. The control involves the full position feedback (the term $-K_{Pj}(q_j - q_j^*)$) plus the pure damping (term $-K_{Dj}\dot{q}_j$). Such simple control is considered appropriate for the purpose of this example.

6.2 Analysis of the results

Figure 5 shows the realized motion in the case of a fairly trained player. His intention (and reference) was to jump, catch the ball, swing with his hand, and throw the ball. According to Figure 5, his attempt was successful. Let us analyze the player's motion in more detail. One can observe several phases of the motion:

- *Phase 1 – takeoff:* Both legs are in contact with the ground accelerating the body upward (Figures 5a–c). This phase ends at 0.108 s. At this instant the legs lose the contact with the ground (Figure 5c).
- From the viewpoint of mechanics the flier (player in this example) has two contacts with an immobile object – both feet are on the ground. A closed chain is formed. Each contact restricts all six relative motions and accordingly creates six reaction forces/torques (twelve reactions in total).

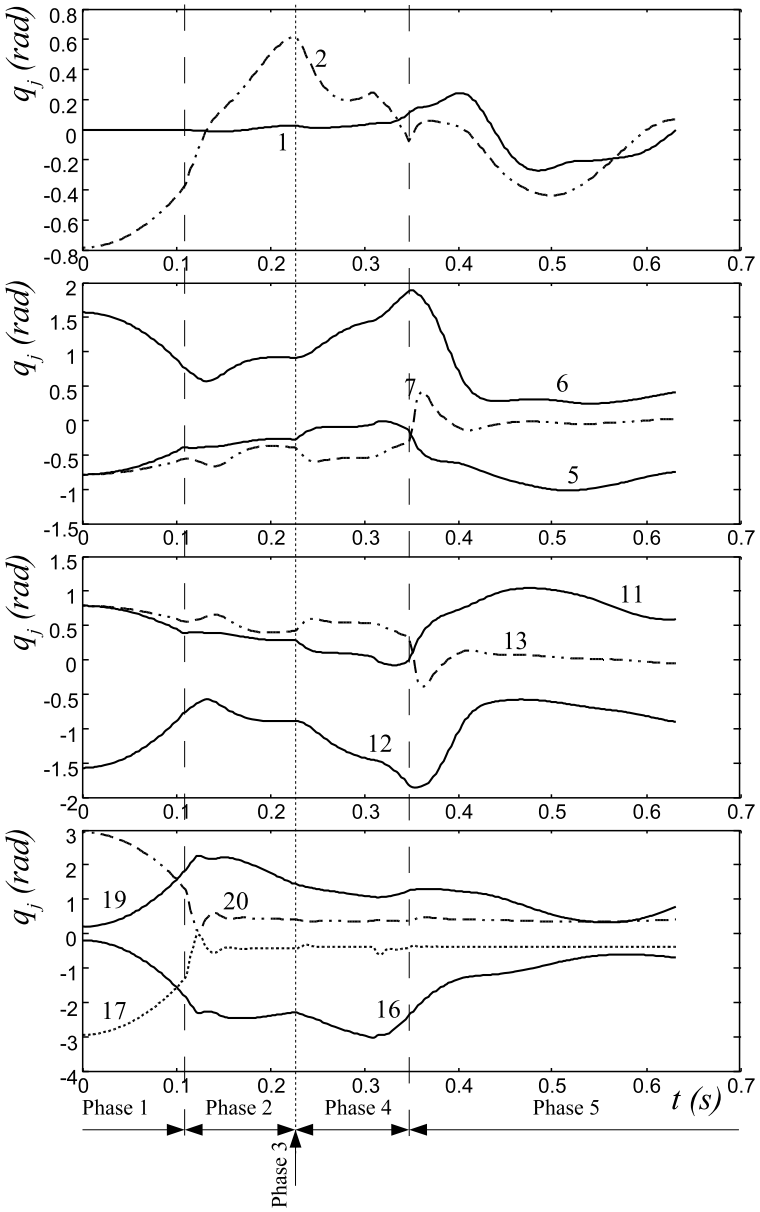

Fig. 7 Time histories of the joint coordinates: $q_j(t)$, $j = 1, \ldots$ (a selected set)

- *Phase 2 – free flight toward the ball*: The player is moving (flying) up while expecting the contact with the ball (Figures 5d–f). The right hand establishes the contact with the ball (catches the ball) at 0.224 s and Phase 2 ends (Figure 5f).
- In this phase, there is no contact with any object; a true flier is considered. The system has a tree structure (no closed chain).

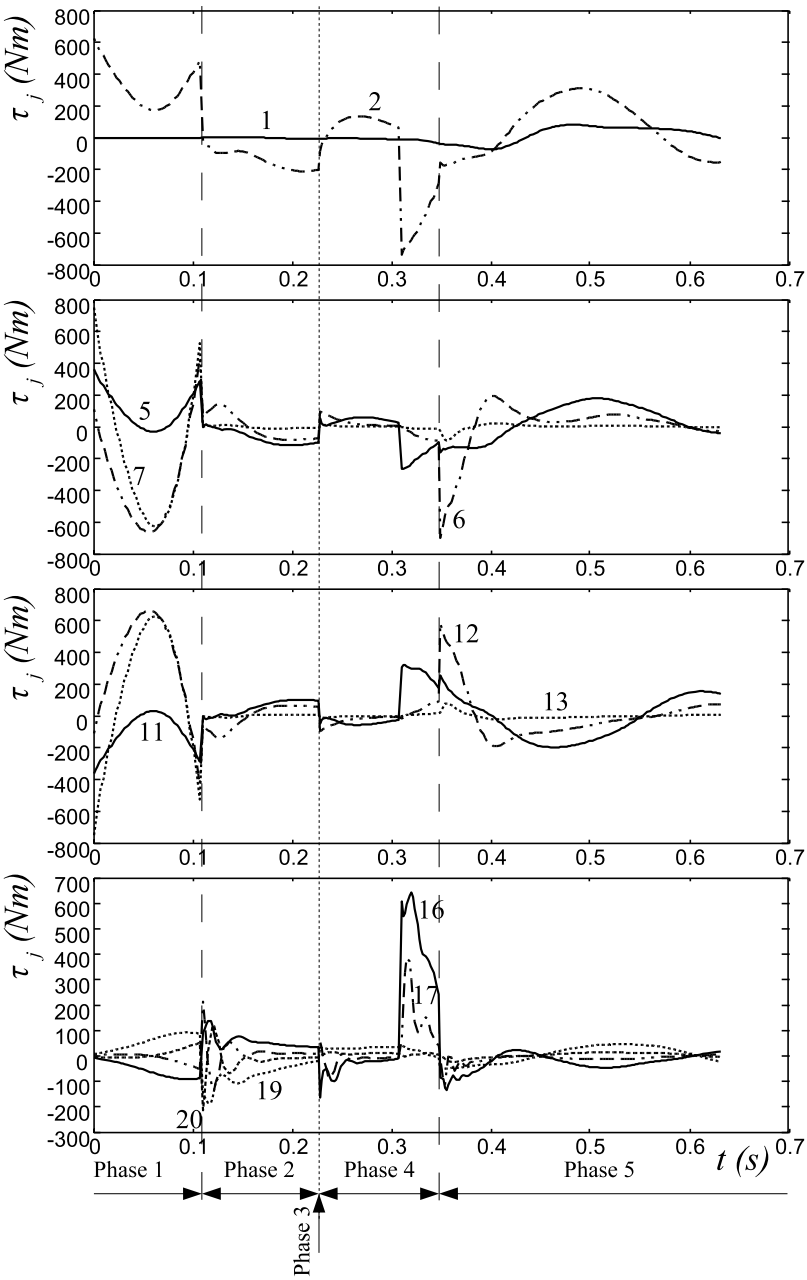

Fig. 8 Time histories of the joint torque: τ_j, $j = 1, \ldots$ (a selected set)

- *Phase 3 – impact*: The contact of the player's hand and the ball always involves an impact effect. It occurs at 0.224 s (Figure 5f). For the current analysis we assume an infinitely short impact.
- The collision between the hand motion and the motion of the object (the ball) will cause an impact. Since the contact will restrict all six relative coordinates, the impact is characterized

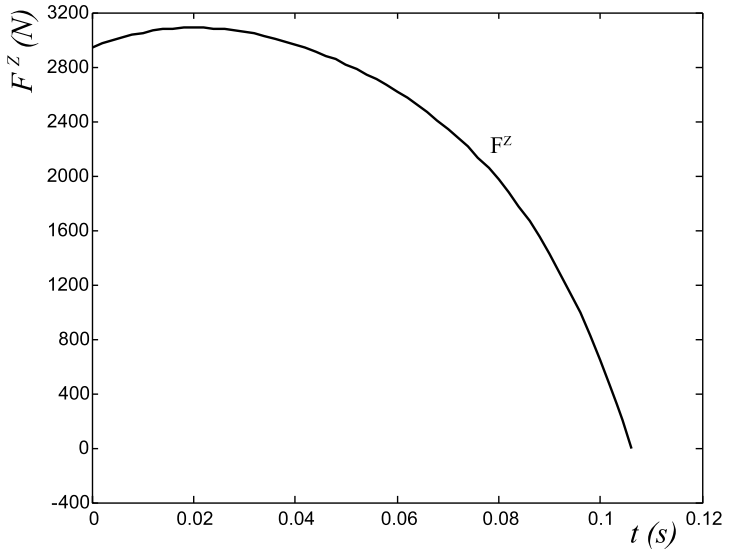

Fig. 9 The launching force – the total vertical contact force between the player's feet and the ground (in Phase 1)

by a six-component momentum. The infinitely short impact generates infinitely large reactions and, accordingly, the instantaneous change in the system velocities. The momentum still has a finite value.

- *Phase 4 – swinging and throwing*: The player swings with his right arm (Figure 5g) and throws the ball (Figure 5h). The ball leaves the player's hand at 0.358 s and Phase 4 ends.
- From the point of view of mechanics, a contact is established between the flier's hand and an external mobile object (the ball). The contact restricts all six relative motions and produces six reaction forces/torques. The contacted object is a separate system (body) that has its own dynamics, now being influenced by the flier (and vice versa).
- *Phase 5 – falling down*: The ball and the player now move separately (Figures 5i–l). The ball has its own trajectory, to hit the ground in front of the goal. The player is falling down (free flying) until landing (he touches the ground at 0.622 s, Figure 5l). The landing is performed correctly, so that the player will not overturn.
- Since there is no contact, a truly free flier is considered again. This lasts until a new impact establishes the contact of the flier's right foot and the ground.

Our simulation stops when the player touches the ground.

Some characteristics of this motion deserve additional attention.

Figures 6 and 7 show the realized motion of the player. Figure 6 presents the motion of the main body – the torso. Time histories $\mathbf{X}(t) = [x(t), y(t), z(t), \theta(t), \varphi(t), \psi(t)]$ are given. Figure 7 presents joint trajectories $q_j(t)$, $j = 1, \ldots$. A selected set of joints is given since not all trajectories are seen equally interesting. One can notice that from phase to phase different motions are dominant.

Figure 8 presents the torques generated at the player's joints: τ_j, $j = 1, \ldots$. A selected set is given. One may see that high torques are present (at relevant joints) during Phase 1 (takeoff) and Phase 4 (swinging). In the swinging phase, it is obvious, as expected, that high torques are not generated all the time. While the arm (with the ball) is moving back, the

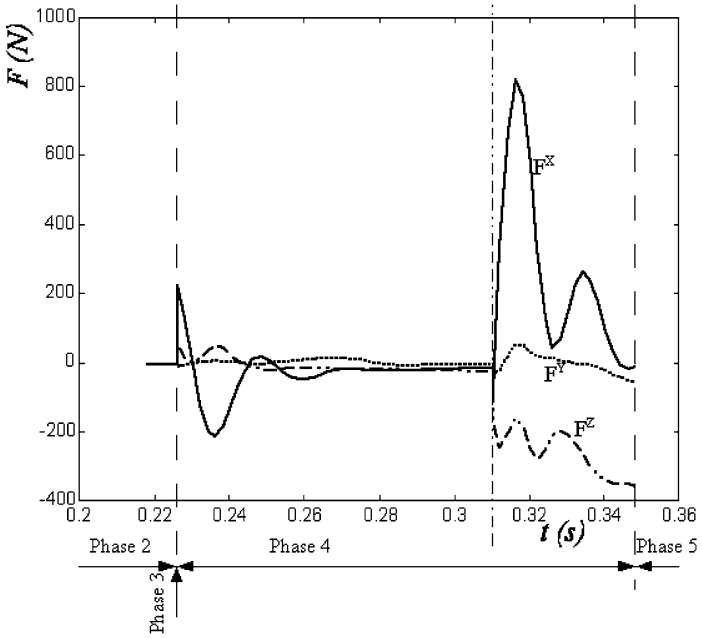

Fig. 10 Contact forces between the hand and the ball (x, y, z indicate the first three axes of the ball-to-hand s-frame)

torques are not high. The arm generates high torques when accelerating the ball in forward direction in order to throw it strongly. It is also evident that almost the complete body (the majority of joints) is engaged in this demanding action (throwing).

We now present the force produced upon the ground during Phase 1 – takeoff. As mentioned, there is a six-component reaction between each foot and the ground. We present the total vertical component (sum for both feet) since it is the force that launches the flier up (Figure 9).

We now concentrate on the contact with the ball. The contact starts with an impact that has a six-component momentum. These components are given in Table 1. Since the impact is considered infinitely short ($\Delta t \to 0$), the infinitely large contact forces/torques will appear causing instantaneous changes in all system velocities. Table 2 shows these changes: first the changes in 20 joint velocities, $\Delta\dot{q}_j,\ j = 1, \ldots, 20$, and then in 6 velocities of the main body (torso), $\Delta\dot{x},\ \Delta\dot{y},\ \Delta\dot{z},\ \Delta\dot{\theta},\ \Delta\dot{\varphi},\ \Delta\dot{\psi}$.

Figure 10 shows the three components of the contact force between the hand and the ball. In the figure, x, y, and z indicate the first three axes of the corresponding ball-to-hand s-frame

Table 1 Impact between the hand and the ball

k	1	2	3	4	5	6
$F_k \Delta t$	1.5291	0.2327	2.2001	−0.0135	0.1723	−0.0041

Note. Six components of the momentum: $k = 1, 2, 3$ correspond to reaction forces along the axes of the local frame and $k = 4, 5, 6$ to reaction moments about these axes. Local x-axis is directed perpendicularly to the hand while the local z is along the hand

Table 2 Impact between the hand and the ball, changes in system velocities

$\Delta\dot{q}_1$	$\Delta\dot{q}_2$	$\Delta\dot{q}_3$	$\Delta\dot{q}_4$	$\Delta\dot{q}_5$	$\Delta\dot{q}_6$	$\Delta\dot{q}_7$	$\Delta\dot{q}_8$
−0.3432	0.4858	−0.5460	0.5308	−0.7093	0.6356	−0.0425	−0.6341
$\Delta\dot{q}_9$	$\Delta\dot{q}_{10}$	$\Delta\dot{q}_{11}$	$\Delta\dot{q}_{12}$	$\Delta\dot{q}_{13}$	$\Delta\dot{q}_{14}$	$\Delta\dot{q}_{15}$	$\Delta\dot{q}_{16}$
−0.5380	0.5073	−0.3060	0.7014	−0.2141	−0.6121	1.8907	−17.8599
$\Delta\dot{q}_{17}$	$\Delta\dot{q}_{18}$	$\Delta\dot{q}_{19}$	$\Delta\dot{q}_{20}$				
3.8313	1.1954	−0.5187	1.0810				
$\Delta\dot{X}$	$\Delta\dot{Y}$	$\Delta\dot{Z}$	$\Delta\dot{\theta}$	$\Delta\dot{\varphi}$	$\Delta\dot{\psi}$		
−0.0502	−0.0166	−0.0153	0.0746	−0.2328	−1.1356		

(s_1, s_2, s_3). Contact torques did not appear interesting. Strong forces appear in the second part of swinging phase (Phase 4), when the ball is accelerated in the forward direction. One can notice that the strongest force is generated in the x-direction and then in z-direction. This comes out from the fact that the acceleration of the ball is mainly along the x axis, and then along negative z.

Figures 11 and 12 show the motion of the ball. Figure 11 presents the three Cartesian coordinates of the ball (of its center), and Figure 12 presents the time derivatives, i.e., the ball velocities. Immobile external Cartesian frame (x, y, z) is used. One can see that in Phase 1 the ball approaches moving with a linear law along the horizontal axis x (in negative direction), meaning constant negative velocity, and a parabolic law along the vertical axis z, meaning a

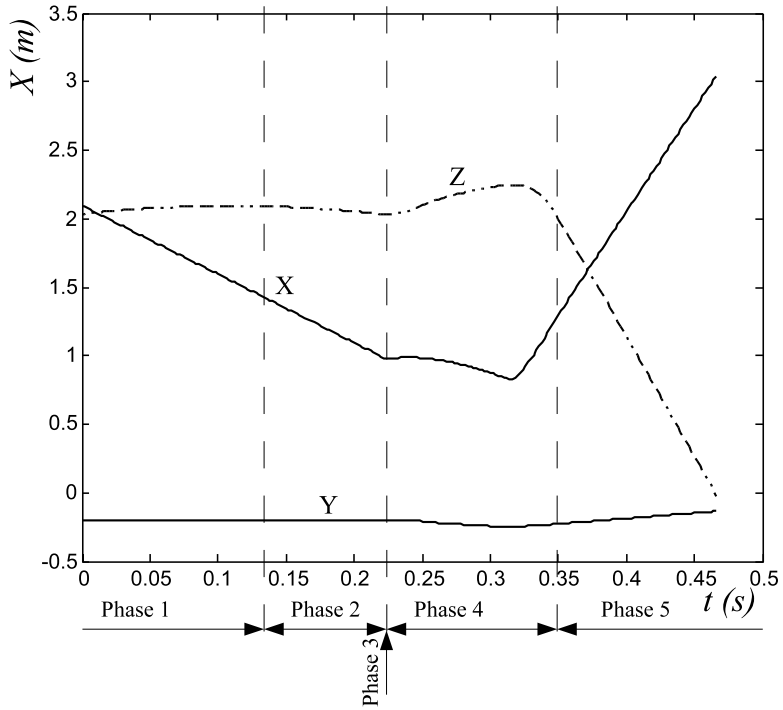

Fig. 11 Time histories of the ball coordinates (motion of its center)

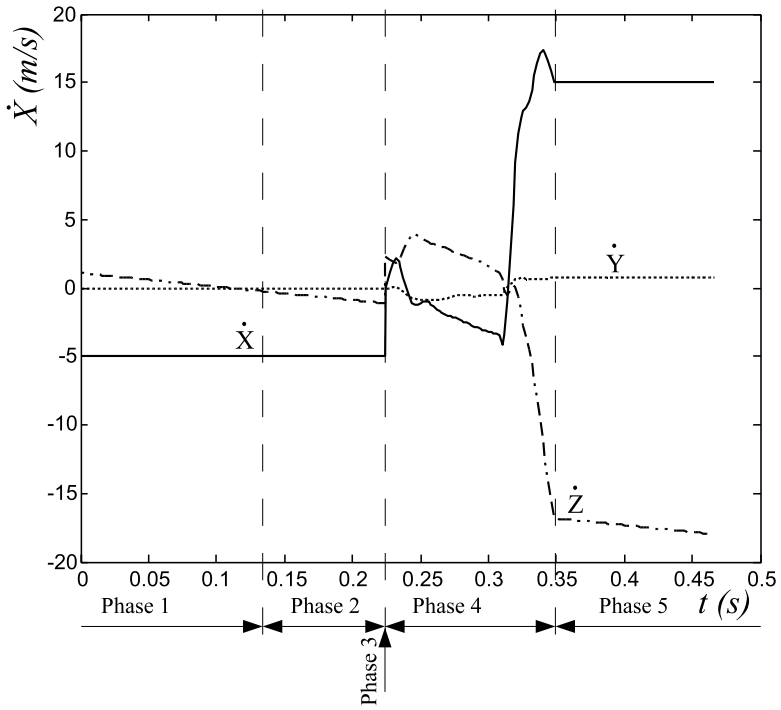

Fig. 12 Time histories of the ball velocities (motion of its center)

constant negative acceleration (gravity constant g). The same happens in Phase 5, but with the positive motion along x. In this phase the parabolic character of z-motion is hard to observe due to high velocity of the ball after throwing. Such motion laws are characteristic for the free motion (when there is no contact).

In Phase 3 – impact – one can notice the sudden change in ball velocities. This is a consequence of the infinitely high contact forces that appear with the infinitely short impact (as explained above). Six components of impact momentum were given in Table 1.

In Phase 4 – swinging – high accelerations in forward (x) and downward (z) directions are present in the second part of this phase, before the ball is actually thrown. Remember that the ball should go forward and down to hit the ground in front of the goal (Figure 4).

A new simulation is made to show the action of insufficiently trained player (clumsy player). This means that his reference motion (learned pattern) is not appropriate. In such case, the local PD regulators can track the reference but cannot prevent the undesired outcome. The motion is shown in Figure 13. During Phases 1–4 (Figures 13a–h) everything seems to go well. However, after throwing the ball (Figure 5i), the player is inclined too much and has an angular momentum in forward direction, and so it is not likely that he will manage to keep the balance. In Phase 5 (Figures 15i–l) the player falls down, and after landing he looses the balance and continues falling by overturning in forward direction. Thus, the final outcome might be successful regarding hitting the goal, but the bad landing makes the entire action inappropriate (clumsy).

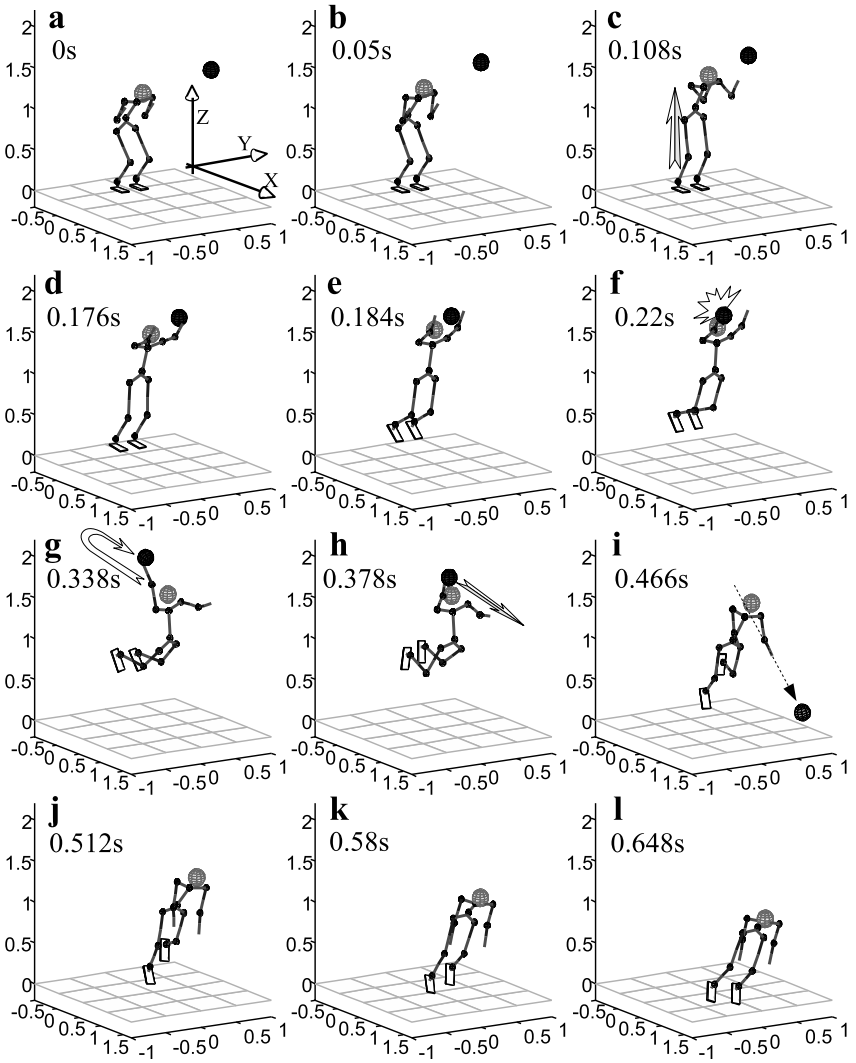

Fig. 13 The "movie" of a clumsy player; after the action he overturns and falls down on the ground

7 Simulation: Example 2

7.1 Configuration and the task

The player configuration used in Example 1 is modified by introducing more complex arms. The new configuration of arms is shown in Figure 14. So, the number of DOFs at the player's joints is now $n = 28$. This was necessary in order to make the player capable of handling the new task (involving closed chain).

The task is selected as a specific action of a goalkeeper in soccer. The ball is moving toward the goalkeeper; he jumps, catches the ball with both hands, moves it toward his waist,

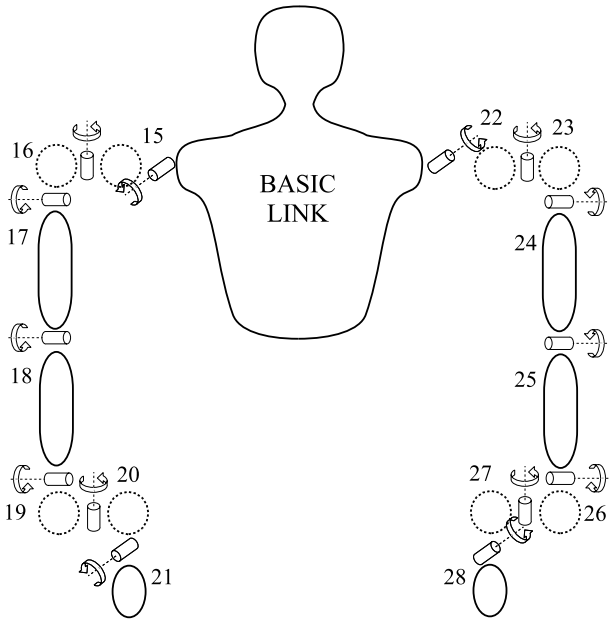

Fig. 14 The new configuration of the human/humanoid arms

and finally lands while holding the ball all the time. In a realistic situation, this would be a learned pattern; we consider this player's motion as a reference and try to realize it by using local PD regulators (as explained in Example 1). For this simulation the reference motion was not measured but synthesized numerically. Here, we will not show the reference but the realized motion only. The ball mass is 450 g and the radius 13 cm.

The complex arm configuration was needed to handle the problem of closed chain dynamics (when holding the ball with both hands). A simpler configuration would be inappropriate, as it would generate infinite contact reactions (forces/torques).

7.2 Analysis of the results

Figure 15 shows the realized motion of the goalkeeper. His intention (and reference) was to jump, catch the ball with both hands, and land while holding the ball. According to Figure 15, his attempt was successful. Let us analyze the goalkeeper's motion in more detail. One can observe several phases of the motion:

- *Phase 1 – takeoff.* Both legs are in contact with the ground accelerating the body upward (Figures 15a–c). This phase ends at 0.108 s. At this instant the legs lose the contact with the ground (Figure 5c).
- From the viewpoint of mechanics, the flier (goalkeeper in this example) has two contacts with an immobile object – both feet are on the ground. A closed chain is formed. Each contact restricts all six relative motions and, accordingly, creates six reaction forces/torques (twelve reactions in total).

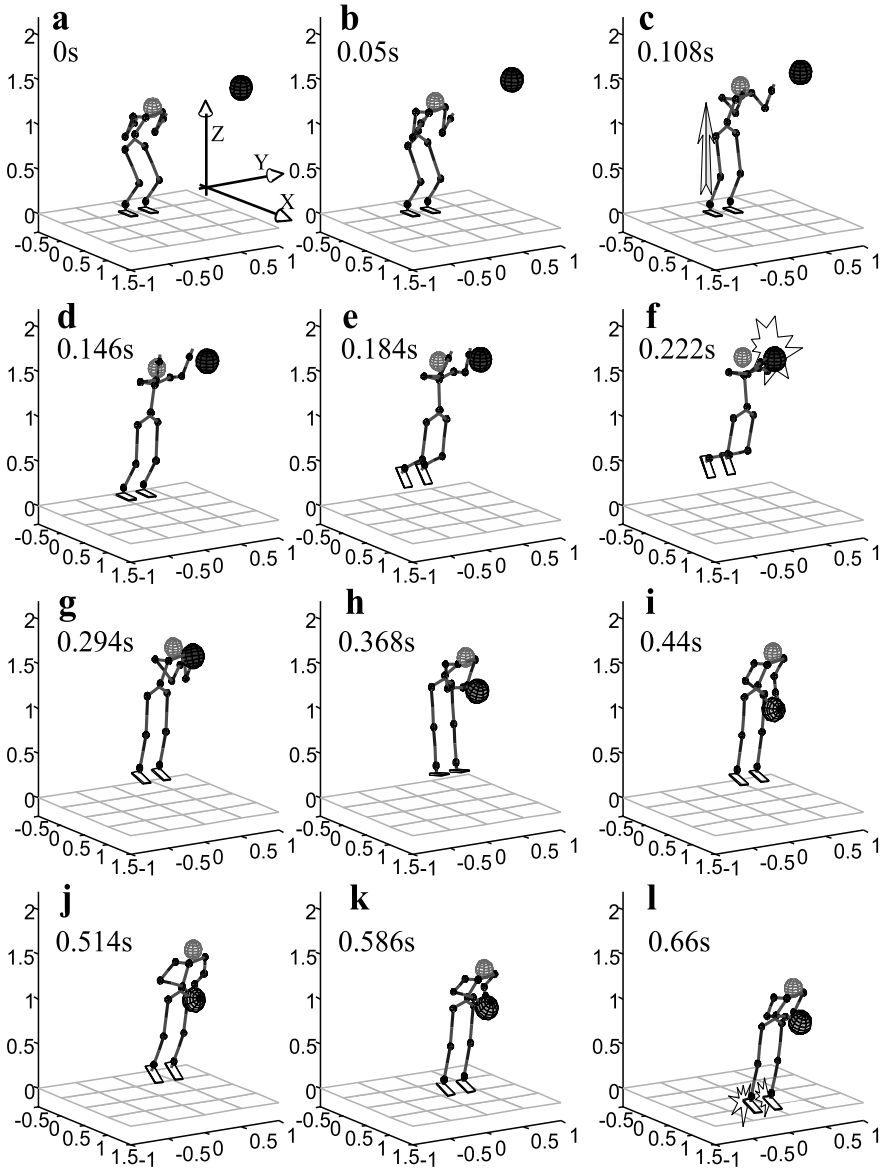

Fig. 15 The "movie" of the human/humanoid goalkeeper motion. Characteristic instants defining the phases of motion are indicated

- *Phase 2 – free flight toward the ball.* The goalkeeper is moving (flying) up while expecting the contact with the ball (Figures 5d–f). Both hands establish the contact with the ball simultaneously (catching the ball) at 0.222 s and Phase 2 ends (Figure 5f).
- In this phase, there is no contact with any object; a true flier is considered. The system has a tree structure (no closed chain).

- *Phase 3 – impact*: The contact of the goalkeeper's hands and the ball always involve an impact effect. It occurs at 0.222 s (Figure 5f). For the current analysis we assume an infinitely short impact.
- The collision between the motion of the hands and the motion of the object (the ball) will cause an impact. The contact with each hand will restrict all six relative coordinates. So, the complex impact is characterized by one six-component momentum for each hand (twelve components in total). Note that the arms holding the ball form a closed chain. The infinitely short impact will generate infinitely large reactions that will cause instantaneous change in the system velocities.
- *Phase 4 – falling down.* The goalkeeper falls down while holding the ball with both hands. In order to guard the ball better, he pulls it toward his waist. So, the flier has two contacts. The ball and the player now move together (Figures 5g–l). The contact with the ground is established at 0.66 *s* (Figure 15l). The landing is performed correctly, so the goalkeeper will not overturn.
- From the viewpoint of mechanics, two contacts are established between the flier's hands and an external mobile object (the ball). Each contact restricts all six relative motions and produces six reaction forces/torques (twelve reactions in total). The arms holding the ball form a closed chain. The contacted object is a separate system (body) that has its own dynamics, now being influenced by the flier (and vice versa). The entire system is falling down until landing.

Our simulation stops when the player touches the ground.

8 Conclusion

The fact that advanced humanoid robots are becoming more and more humanlike in their shape and motion start to erase the border between the two disciplines: robotics and biomechanics. Today's robots, including humanoids, are still "machines," meaning that they involve just one-degree-of-freedom joints connecting rigid links. This comes out from the fact that actuator technology still offers just "classical" stator-rotor motors. However, it is expected that the development of artificial muscles will lead to robots of more humanlike shape that will be strongly inspired by human skeleton. At that moment, the mentioned border will finally disappear.

Even at this stage of humanoid-robot development, it is justified to encourage the further research that lies between robotics and biomechanics of human motion. Both disciplines benefit from such work. Robotics learns about how humans resolve some important problems in motion, like redundancy, coordination, stability, etc. On the other hand, sophisticated mathematical models developed for advanced robots may become a very useful tool for biomechanics to simulate human motion in different activities of everyday life, sport, etc. By simulation, the motion may be improved to become more effective regarding some criterion. In one example a sportsman could be retrained to run faster with reduced effort. In the other example the learned motion pattern for tennis service could be modified so as to keep the positive effects and redistribute (in a better way) the load upon the shoulder and elbow, thus reducing the possibility of hurt.

This paper proposed a general approach to humanoid-robot motion, applicable to any motion task: walking, running, manipulation in industrial environment, gymnastics, basketball, soccer, handball, tennis, etc. It was our idea to promote the method as a tool for biomechan-

ics as well. That is why we used term "human/humanoid motion," and both examples were selected as sporting motions.

The extreme complexity of the problem of modeling biological systems stems from the complexity of the mechanical structure and actuation. That is why we started from an approximation – a complex body of a humanoid robot. Since the developed algorithm for the dynamic modeling and the corresponding software do not make limits to the complexity of the humanoid body, we see them a useful tool for biomechanics as well – an appropriate approximation of human body is achieved. At the same time a good foundation is set to develop a truly biological model, as the next research step. In order to avoid unnecessarily complex problem, we will apply "biological modeling" to key joints only. For a particular action (in everyday life or in sport), key joints will be located and remodeled to agree with their biological structure.

Appendix A: Model parameters

			Moments of inertia		
Link (name)	Length (m)	Mass (kg)	J_x	J_y	J_z
Trunk+head	0.60	30.85	0.1514	0.137	0.0283
Pelvis	0.15	6.96	0.007	0.00565	0.00627
Right thigh	0.44	8.41	0.0114	0.012	0.003
Right shank	0.42	3.21	0.00393	0.00393	0.00038
Right foot	0.10	1.53	0.0006	0.00055	0.00045
Left thigh	0.44	8.41	0.0114	0.012	0.003
Left shank	0.42	3.21	0.00393	0.00393	0.00038
Left foot	0.10	1.53	0.0006	0.00055	0.00045
Right upper arm	0.308	2.07	0.002	0.002	0.00022
Right lower arm	0.264	1.14	0.0025	0.00425	0.00014
Right hand (goalkeeper only)	0.1	0.35	0.0005	0.001	0.00003
Left upper arm	0.308	2.07	0.002	0.002	0.00022
Left lower arm	0.264	1.14	0.0025	0.00425	0.00014
Left hand (goalkeeper only)	0.1	0.35	0.0005	0.001	0.00003

References

1. http://www.robocup.org/ home page of RoboCup association
2. Fukuda, T., Michelini, R., Potkonjak, V., Tzafestas, S., Valavanis, K., Vukobratovic, M.: How far away is "artificial Man". IEEE Robotics and Automation Magazine, March 2001, pp. 66–73 (2001)
3. Potkonjak, V., Vukobratovic, M.: A generalized approach to modeling dynamics of human and humanoid motion. Intl. J. Humanoid Robotics (World Scientific publ.) **2**(1), 1–24 (2005)
4. Potkonjak, V., Vukobratovic, M., Babkovic, K., Borovac, B.: General model of dynamics of human and humanoid motion: Feasibility, potentials and verification. Int. J. Humanoid Rob. **3**(1), 21–48 (2006)
5. Vukobratovic, M., Borovac, B.: Zero-Moment point, thirty-five years of its Life. Int. J. Humanoid Rob. **1**(1), 157–173 (2004)
6. Vukobratovic, M., Juricic, D.: Contribution to the synthesis of the biped gait. IEEE Trans. Bio-Med. Eng. **BME16**(1), 1–6 (1969)
7. Vukobratovic, M., Stepanenko, J.: On the stability of anthropomorphic systems. Math. Biosci. **15**, 1–37 (1972)

8. Ken'ichiro, N., et al.: Integrated motion control for walking, jumping and running on a small bipedal entertainment Robot. In: Proceedings of the IEEE International Conference on Robatics, & Automation, pp. 3189–3194 (2004)
9. Blajer, W., Czaplicki, A.: Modeling and inverse simulation of somersaults on the trampoline. J. Biomech. **34**, 1619–1629 (2001)
10. Blajer, W., Czaplicki, A.: Contact modeling and identification of planar somersaults on the trampoline. Mult. Sys. Dyn. **10**, 289–312 (2003)
11. Vukobratovic, M., Potkonjak, V., Tzafestas, S.: Human and humanoid dynamics – From the past to the future. J. Intell. Robotic Sys. **41**(1), 65–66 (2004)
12. So, B.R., Yi, B.J., Kim, W.K.: Analysis of impulse in sports action: Towards Robot sports. ASME J. Dyn. Int. Sys. **3**(1), 121–129 (2002)
13. So, B.R., Yi, B.J., Sang-Rok, O., Kim, Y.S.: Landing motion analysis of human-body model considering impact and ZMP condition. In: Proceeding of 2004 IEEE/RSJ International Conference on Intelligent Robots and Systems, Sendai, Japan, pp. 1972–1978 (2004)
14. Vukobratovic, M., Potkonjak, V., Matijevic, V.: Dynamics of Robots with contact tasks, research monograph. Kluwer Academic Publishers (2003)